BOLLETTINO DI GEOFISICA TEORICA ED APPLICATA VOL. 40, N. 3-4, pp.387-394; SEP.-DEC. 1999

A global grid of high-resolution gravity anomalies based on Geosat and ERS-1 altimetry

M. RENTSCH, TH. GRUBER and M. ANZENHOFER

GeoForschungsZentrum, Potsdam, Germany

(Received October 4, 1998; accepted August 5, 1999)

Abstract. A global high-resolution marine gravity field was derived by processing upgraded altimeter data from the Geodetic Missions of Geosat (April 1985 to September 1986) and ERS-1 (April 1994 to March 1995). After the generation of crossover points, along-track sea surface derivatives were calculated at each 1-Hz altimeter point. The long-wavelength part of the gravity field GFZ95A was first removed from the sea surface heights. The first derivatives of the sea surface profiles in direction of the crossing tracks were interpolated at the altimeter points by using the slope information from the crossover points. The residual sea surface slopes were converted to east and north vertical deflections, which were then interpolated onto a regular grid with a 2' by 2' resolution. By means of the 2-dimensional Fast-Fourier transformation (FFT) the deflections were loss-pass filtered and the residual gravity anomalies were calculated in subsquares. After the inverse FFT of each subsquare, the global anomaly grid was merged and finally, the long-wavelength part was added to recover the complete marine gravity field. Quality tests were performed by comparing the altimetry derived anomalies with anomalies from the gravity maps of several authors and in addition, with validated and adjusted shipboard gravity data.

1. Introduction

The knowledge of a high-accuracy and detailed gravity field over all ocean basins is a basic tool for various geophysical applications, e.g. the prediction of seafloor depth and investigations on the age and the structure of the oceanic lithosphere. Starting with the Geos-3 mission in 1975, global distributed gravity anomalies could be generated for the first time from altimeter measurements (Rapp, 1979). The follow-on altimeter missions then provided

Corresponding author: M. Rentsch; GeoForschungsZentrum Potsdam (GFZ), c/o DLR Oberpfaffenhofen, D 82234 Wessling, Germany; phone: + 49 8153281267, fax: +49 8105 8713; e-mail: rentsch@gfz-potsdam.de

an increase in coverage, resolution and accuracy, but the full potential of altimetric derived gravity anomalies was achieved at first by making use of the high-density coverage of the Geosat and ERS-1 Geodetic Missions. The method of computing gravity anomalies from vertical deflections using the FFT approach is well-known (Haxby et al., 1983) and was refined in the following by various works, e.g. Sandwell (1992), Olgiati et al. (1994), Sarrailh et al. (1997), Sandwell and Smith (1997), Andersen et al. (1998), Hwang et al. (1998). The present paper is focussed on a method which is a combination of the approaches used by Sandwell (1992) and Olgiati et al. (1994). A global map of marine gravity over the oceans was produced, named GFZ98 gravity grid in the following. For the evaluation of the results a test area along the Mid-Atlantic Ridge (30.5°-36.5°S) was selected which was already investigated by Neumann et al. (1993) and Olgiati et al. (1994).

2. Data

UPGRADED ERS-1 OPRS. - From ERS-1's launch in July 1991, nearly 5 years of altimeter data were collected. For the generation of operational high-level geophysical products the ocean product data records of ERS-1 were received from the French Processing and Archiving Facility for ERS (F-PAF) and were systematically upgraded by GFZ (Gruber et al., 1997). This process included the application of a time bias of +1.5 ms and the remerging of the orbital height based on the PGM055 gravity model (Anzenhofer and Gruber, 1997). For the computation of corrected altimeters ranges some of the standard geophysical quantities and path delay corrections were replaced by enhanced model corrections, e.g. the FES95.2 ocean tide model (Le Provost et al., 1998) and the IRI95 ionospheric model (Bilitza, 1997). During the Commissioning Phase of ERS-2 against ERS-1, two additional internal corrections (USO drift, SPTR correction) were found and also applied.

JGM-3 ENHANCED GEOSAT GDRS. - Geosat was launched in March 1985 and collected global altimeter data until October 1989. The 1997 release of Geosat GDRs represents the first globally distributed and consistent data set for the entire mission. The orbit processing was refined by NASA Goddard Space Flight Center using the JGM-3 gravity model. Moreover, nearly all geophysical corrections were enhanced and reanalyzed. Second order corrections (e.g. global inverse barometer correction, USO drift and internal calibration) were also included. These improvements led to decrease in the global crossover rms down to 13 cm during the first 3.5 years of the mission (Lillibridge and Cheney, 1997).

3. Generation of high-resolution marine gravity

A global high-resolution marine gravity field was derived by processing the Geodetic Missions of Geosat and ERS-1. The main processing steps consist of crossover generation, along-track sea surface slope estimation, the generation of vertical deflection grids and finally, the generation of gravity anomalies by the FFT approach.

Table 1 - Editing criteria for range measurements.

Item	Unit	Minimum	Maximum
No. of valid 20-Hz (10-Hz) measurements	mm	17 (8)	20 (10)
Standard deviation of 1-Hz altimeter range	mm	1	100
Significant wave height	cm	0	800
Standard deviation of 1-Hz SWH	cm	1	100
Backscatter coefficient	0.01 dB	700	2300
Ocean tide	mm	-2500	2500
Solid Earth tide	mm	-1000	1000
Ionospheric correction	mm	-200	-1
Dry tropospheric correction	mm	-2400	-2100
Meteorological wet tropospheric correction	mm	-600	-1
Radiometer wet tropospheric correction	mm	-600	-1

3.1. Crossover generation

The crossover generation is the basis for the following processing step in which the exact crossover locations are needed as anchor points. The crossover generation is a standard procedure and the description of the method can be found in Anzenhofer et al. (1996). For Geosat and ERS-1 all possible crossovers within the time periods of the Geodetic Missions were generated, hence ascending and descending crossover times differ by a maximum time difference of 549 days for Geosat and 344 days for ERS-1, respectively. Crossovers with an absolute sea surface height difference exceeding 40 cm were not considered.

3.2. Computation of reduced sea surface heights and derivation of sea surface slopes

At first, all valid ocean altimeter ranges were carefully edited according to the criteria given in Table 1. The standard deviation of a 1-Hz altimeter range results from the division of the standard deviations of the 20-Hz (10-Hz for Geosat) range estimates by the square root of the number of valid 20-Hz (10-Hz) measurements. For ERS-1, the standard deviation of a 1-Hz significant wave height is obtained from the standard deviations of the 20-Hz significant wave height estimates in the same way. This field is not included in the Geosat GDRs. For ERS-1 in general, the microwave radiometer wet tropospheric correction was applied, only in case of its absence the meteorological wet tropospheric correction was taken. Geosat was not supplied with a microwave radiometer, thus 3 model-based wet tropospheric corrections are provided in one Geosat GDR. In this paper, the wet tropospheric correction was taken from the NCEP/NCAR reanalysis model (Kalnay et al., 1996).

Along-track sea surface heights were calculated and were rejected if the absolute difference to the mean sea surface from the MSS95A model (Anzenhofer et al., 1996) exceeded 1.0 m. The long-wavelength geoid part (up to degree 70 where the coefficients were cosine tapered between degrees 50 and 70) was derived from the gravity model GFZ95A (Gruber et al., 1996) and

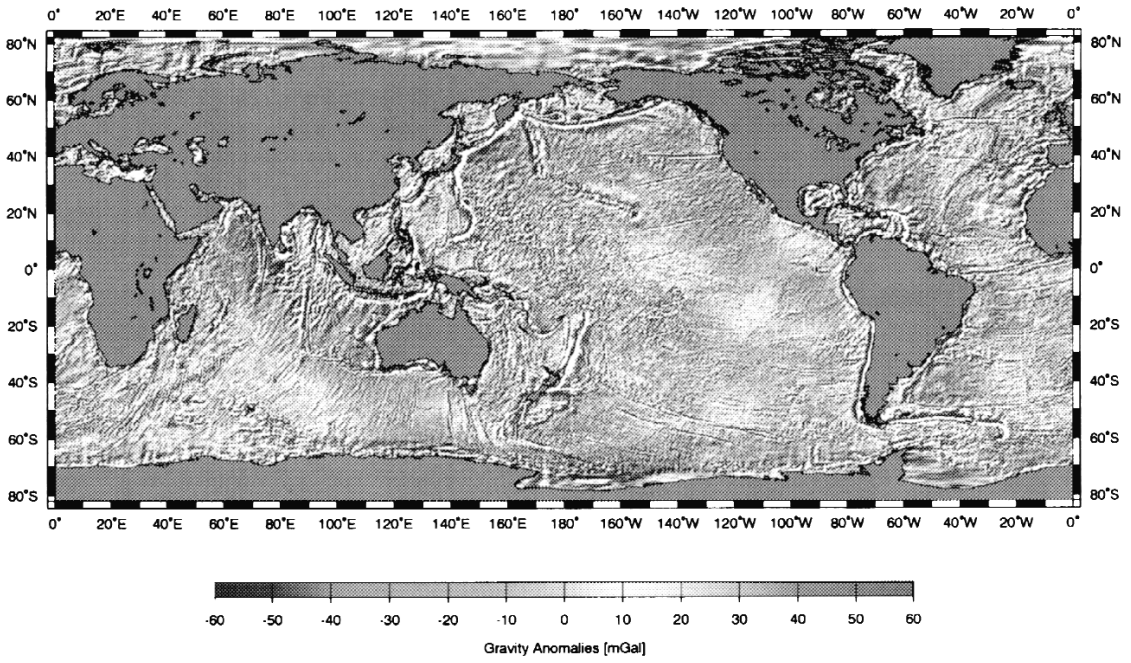

Fig. 1 - Global Marine Gravity From Geosat and ERS-1 Altimetry.

removed from the sea surface profiles. This is necessary to reduce the error due to the assumption of the flat-earth approximation on which the FFT is based. In a first step, the generation of sea surface slopes was performed for the ascending and descending arcs at all crossover locations. After having applied a 5-sigma criterion to the slope values, the minimum and maximum values of the first derivatives were taken as limits for the second step, in which again, all ascending and descending arcs were investigated. Herein first derivatives were computed in the along-track direction at each altimeter point, then crossover events were located and now the derivatives in direction of the crossing tracks were interpolated at each altimeter point of the ascending arc. In the same way, all descending arcs were processed which finally led to first derivatives in both the along-track and the cross-track direction at each altimeter point.

3.3. From sea surface slopes to vertical deflections

Using the formulas (B4), (B5) and (B11) given by Sandwell and Smith (1997), the east and north deflection components were calculated from the sea surface slopes. Because the influence of the stationary sea surface topography was already filtered out, sea surface slopes can be assumed to be identical to geoid slopes. The exact ground track velocities which also appear in these formulas were calculated using orbit information. Finally, the vertical deflections were interpolated onto a regular 2' by 2' grid by means of a weighted mean algorithm. Several tests were performed by varying the radius of the influence circle and the half weight width in order

to seek the best transfer of the high-resolution signal to the grids as possible. We obtained the best results with a radius of 3' and a half weight width of 25%.

3.4. From vertical deflections to gravity anomalies

The basic formalism to compute gravity anomalies from vertical deflections by means of the 2-dimensional FFT can be found in Appendix A of Sandwell and Smith (1997). Merging the approximated Bruns formula and Laplace's equation yields a gravity-geoid relationship between the vertical gravity gradient and the first derivatives of the east and north vertical deflection. The gravity anomaly Δg fullfills the Laplace equation and the upward continuation formula rates Δg at a certain elevation z and on the geoid ($z=0$), in the space domain as well as in the frequency domain. Taking the first derivative of z at $z=0$ now results in the relationship of the Fourier transformed gravity anomaly as sum of the Fourier transformed vertical deflection components.

After the Fourier transformation of the vertical deflection grids to the frequency domain, the calculantion of Δg was performed in subareas of 128 by 128 grid points surrounded by 100% zero-padding. A 2-dimensional low-pass filter was applied at this tep to each subarea by rejecting all frequencies with wavelengths shorter than 12'. In order to suppress truncation effects at the edges of a subarea, only an inner zone of 64 by 64 grid cells was considered. After the inverse Fourier transformation of each subsquare, the original area was reconstructed by a padding procedure. Finally, the long-wavelength gravity anomalies were added back to the result to obtain the complete gravity field.

4. Comparisons

The validation of the GFZ98 gravity grid was performed in an 5° by 6° area along the Mid-Atlantic Ridge (17° W, 30.5° S to 12° W, 36.5° S) by comparison with the following data sets:

- SIO95: Free-air anomalies from the 2' by 2' Mercator projected gravity map (version 7.2) of Smith and Sandwell (1995);
- KMS97: Free-air anomalies from the 3.75' by 3.75' gravity map of Andersen and Knudsen (1997). The method of computing gravity anomalies differs from the method in the SIO95 gravity grid;
- KMS98: Free-air anomalies from the 2' by 2' gravity map of Andersen et al. (1998);
- Marathon, Plume: Two data sets of adjusted and validated shipboard free-air gravity anomalies from the Marathon 10&13 cruises (1984-85) and the Plume 4&5 cruises (1990) of the R/V Thomas Washington (Neumann et al., 1993). According to Neumann (pers. comm.) the Plume data set is the better of the two;
- Knorr: Shipboard gravity measurements from the 1996 GPS navigated cruise of the R/V Knorr. Crossover analyses were performed with the Plume 4&5 cruises (Neumann, pers. comm.).

Before comparing the SIO95 and KMS97 gravity grids with the GFZ98 solution, the gravity anomalies were also interpolated onto 2' by 2' equidistant point value grids by means of the

Table 2 - Comparisons of the GFZ 98 gravity grid with external data sets.

	Min. [mGal]	Max. [mGal]	Mean [mGal]	RMS [mGal]	#Points
GFZ98-SI095	-25.53	22.35	-1.20	4.03	27331
GFZ98-KMS97	-24.53	20.53	-0.75	3.93	27331
GFZ98-KMS98	-24.91	21.88	-0.70	4.10	27331
GFZ98-Marathon	-23.12	22.44	-0.33	7.42	28885
GFZ98-Plume	-20.68	20.42	0.09	6.40	47967
GFZ98-Knorr	-21.93	18.12	-2.20	6.13	105452
SI095-Marathon	-18.54	19.08	0.29	6.16	29072
SI095-Plume	-16.32	18.42	1.03	5.47	48288
SI095-Knorr	-15.62	15.12	-0.21	5.03	108659
KMS97-Marathon	-22.58	23.66	0.54	7.55	28876
KMS97-Plume	-21.39	24.57	1.77	7.28	48073
KMS97-Knorr	-22.15	20.52	-0.86	7.01	106738
KMS98-Marathon	-18.03	18.04	0.01	5.88	28898
KMS98-Plume	-15.80	17.52	1.00	5.27	48063
KMS98-Knorr	-16.28	14.81	-0.70	5.12	106820

weighted mean algorithm. For the comparisons of the GFZ98 gravity grid with the shipboard gravity, the anomalies were bilinear interpolated at the point locations of the shipboard measurements. The comparisons between the gravity anomalies of SIO95, KMS97 and the shipboard gravity were performed in the same way, but using the original data in order to avoid the effects resulting from the gridding process. In general, a 3-sigma cirterion was applied to the statistics.

Table 2 shows a correspondence of the GFZ98 gravity grid with the external grids around -1 mGal mean and 4 mGal rms difference. The comparison of the GFZ98 gravity grid with the shipboard gravity data reveals a better agreement than the KMS97 grid, and higher rms differences of around 1.2 mGal with respect to the SIO95 and KMS98 solutions. The comparison of the KMS98 grid with the Marathon, Plume and Knorr data outlines the excellent quality of this data set in this area, and also demonstrates the great improvement with respect to the older KMS97 gravity grid. In addition, the statistics confirm the assumption given by Knudsen (pers. comm.) that the KMS98 grid yields slightly better results than the SIO95 gravity grid.

5. Conclusions and outlook

A global grid of high-resolution marine gravity was computed by means of 2-dimensional Fast-Fourier transformation from vertical deflection grids which were generated on the basis of along-track sea surface slopes. By this method, vertical deflections were calculated at

measurement points and then interpolated without any crossover adjustment or orbit error analysis. Comparing the GFZ98 solution with validated data sets of shipboard gravity offered a better correspondence than the KMS97 solution, but led to slightly worse results with respect to the SIO95 and KMS98 gravity grids.

Further improvements can be expected by refining the algorithms for the determination and interpolation of vertical deflections, e.g. given by Hwang and Parsons (1996). In addition, the retracking of Geosat and ERS-1 waveforms will retain more high-resolution altimeter ranges near coastlines and around small islands. In general, future applications will be focussed on smaller regions in combination with shipboard gravity measurements and airborne gravity campaigns, e.g. the AGMASCO project (Timmen et al., 1998).

Acknowledgements. We wish to thank Greg Neumann for providing the validated shipboard gravity data sets of the Marathon 10&13, the Plume 4&5 and the Knorr cruises and furthermore, we thank David Sandwell for providing an exabyte with the 2´ by 2´ gravity anomalies and the access software. The marine gravity plot was generated with GMT-3 (Wessel and Smith, 1995).

References

Anderson O. B. and Knudsen P.; 1997: *Global gravity field from the ERS-1 and GEOSAT Geodetic Mission altimetry.* Journal of Geophysical Research, **103**, 8129-8137.

Anderson O. B., Knudsen P., Kenyon S. and Trimmer R.; 1998: *Recent improvements in the KMS98 Global Marine Gravity Field.* This issue.

Anzenhofer M. and Gruber Th.; 1997: *Fully reprocessed ERS-1 altimeter data from 1992 to 1995: Feasibility of the detection of long term sea level change.* J. Geophy. Res., **103**, 8089-8112.

Anzenhofer M., Gruber Th. and Rentsch M.; 1996: *Global high resolution Mean Sea Surface based on ERS-1 35- and 168-day cycles and TOPEX data.* In: R. Rapp, R. S. Nerem, A. Cazenave (eds) Global Gravity Field and its Temporal Variations, International Association of Geodesy Sumposia, Vol. 116; Springer Berlin Heidelberg New York, pp. 208-217.

Bilitza D.; 1997: *International reference ionosphere-status 1995/96.* Advances in Space Research, **20**, 1751-1754.

Gruber Th., Anzenhofer M. and Rentsch M.; 1996: *The 1995 GFZ High Resolution Gravity Model.* In: R. Rapp, R. S. Nerem, A. Cazenave (eds); Global Gravity Field and its Temporal Variations, International Association of Geodesy Syumposia, Vol. 116; Springer Be lin Heidelberg New York, pp. 61-70.

Gruber Th., Anzenhofer M. and Rentsch M.; 1997: *Improvements of D-PAF Altimeter Products.* In: Proc. 3rd ERS Symp. on Space at the Service of our Enviroment (ESA SP-414, 3 Vols., May 1997), 1749-1752.

Haxby W. F., Karner G. D., LaBrecque J. L. and Weissel J. K.; 1983: *Digital Images of Combined Oceanic and Continental Data Sets and Their Use in Tectonic Studies.* EOS Transactions AGU, **64**, 995-1004.

Hwang C., Kao E. C. and Parsons B.; 1998: *Global derivation of marine gravity anomalies from Seasat, Geosat, ERS-1 and Topex/Poseidon altimeter data.* Geophysical Journal International, **134,** 449-459.

Kalnay E. et al.; 1996: *The NCEP/NCAR 40-year Reanalysis Project.* Bull. Am. Meteor. Soc., **77**, 437-471.

Le Provost C., Lyard F., Molines J. M., Genco M. L. and Rabilloud F.; 1998: *A hydrodynamic ocean tide model improved by assimilating a satellite altimeter-derived data set.* Journal of Geophysical Research, **103**, 5513-5530.

Lillibridge J. and Cheney R. E.; 1997: *The Geosat Altimeter JGM-3 GDRs on CD-ROM.* User handbook, NODC Laboratory for Satellite Altimetry, Silver Spring, Maruyland, 20 pp.

Neumann G. A., Forsyth D. W. and Sandwell D. T.; 1993: *Comparison of marine gravity from shipboard and high-density satellite altimetry along the Mid-Atlantic ridge, 30.5°-35.5° S.* Geophysical Research Letters, **20**, 1639-1642.

Olgiati A., Balmino G., Saraillh M. and Greeen C. M.; 1994: *Gravity Anomalies From Satellite Altimetry: Comparisons Between Computation via Geoid Heights and Deflections of the Vertical.* Bulletin Geodesique, **69**, 252-260.

Rapp R. H.; 1979: *Geos 3 Data Processing for the Recovery of Geoid Undulations and Gravity Anomalies.* J. Geophy. Res., **84**, 3784-3792.

Sandwell D. T.; 1992: *Antarctic marine gravity field from high-density satellite altimetry;* J. Geophy. Res., **109**, 437-448.

Sandwell D. T. and Smith W. H. F.; 1997: *Marine gravity anomaly from Geosat and ERS-1 altimetry.* J. Geophy. Res., **102**, 10 039-10 055.

Sarrailh M., Balmino G. and Doublet D.; 1997: *The Artic and Antarctic oceans gravity field from ERS-1 altimetric data.* In: J. Segawa, H. Fujimoto, S. Okubo (eds) Gravity, Geoid and Marine Geodesy. International Association of Geodesy Symposia, Vol. 117, Springer Berlin Heidelberg, pp. 437-444.

Smith W. H. F. and Sanwell D. T.; 1995: *Marine gravity field from declassified Geosat and ERS-1 altimetry (Abstract).* EOS Transactions AGU, 76 (Supplement), G42A-02.

Timmen L., Bastos L., Forsberg R., Gidskehaug A., Hehl K. and Meyer U.; 1998: *Establishment of an Airborne Geoid Mapping System for Coastal Oceanography (AGMASCO).* Submitted for publication in the symposium volume of the 3rd European Marine Science and Technology Conference, 23-27 May, 1998, Lisbon, Portugal.

Wessel P. and Smith W. H. F.; 1995: *New Version of the Generic Mapping Tools Released.* EOS Transactions AGU, **76**, 329 pp.